Supporting Information

Optimizing Pore Structure in Silicon-Carbon Anodes: The Impact of Micropore and Mesopore Ratios on Electrochemical Performance

Xiao Mu [a], Xintong Xu [b], Haibang Xu [b], Tao Huang [a]*, Aishui Yu [a, b]*

[a.] *Department of Chemistry, Collaborative Innovation Center of Chemistry for Energy Materials, Shanghai Key Laboratory of Molecular Catalysis and Innovative Materials, Institute of New Energy, Fudan University, Shanghai 200438, China*

[b.] *Laboratory of Advanced Materials, Fudan University, Shanghai 200438, China*

$$SiH_4 \rightarrow Si + 2H_2 \quad \textbf{(Eq. S1)}$$

$$C_2H_2 \rightarrow 2C + H_2 \quad \textbf{(Eq. S2)}$$

$$\text{Micropore Fraction } (\%) = \frac{S_{t-plot}}{S_{BET}} \quad \textbf{(Eq. S3)}$$

$$Weight(Si)\ \% = \frac{W_f}{W_i} \times \frac{28.09}{60.08} \times 100\ \% \quad \textbf{(Eq. S4)}$$

Derivation of the Silicon Content Calculation Formula

During TGA in an oxygen atmosphere, assuming that carbon is completely oxidized and lost as CO_2, whereas elemental silicon is oxidized to form SiO_2.

The molar masses are:

Si: 28.09 g/mol

SiO_2: 60.08 g/mol

Let $\mathbf{W_i}$ be the initial weight (200 °C) and $\mathbf{W_f}$ be the final weight (1300 °C) after oxidation.

Assuming the mass fraction of silicon is **x**, after oxidation, silicon contributes:

$$\mathrm{W_f} = \mathrm{x} \times \mathrm{W_i} \times \frac{60.08}{28.09}$$

Thus, the silicon mass fraction is calculated as:

$$\mathrm{x} = \frac{\mathrm{W_f}}{\mathrm{W_i}} \times \frac{28.09}{60.08}$$

Expressed as a percentage, the silicon content is:

$$Weight(Si)\ \% = \frac{W_f}{W_i} \times \frac{28.09}{60.08} \times 100\ \%$$ **(Eq. S4)**

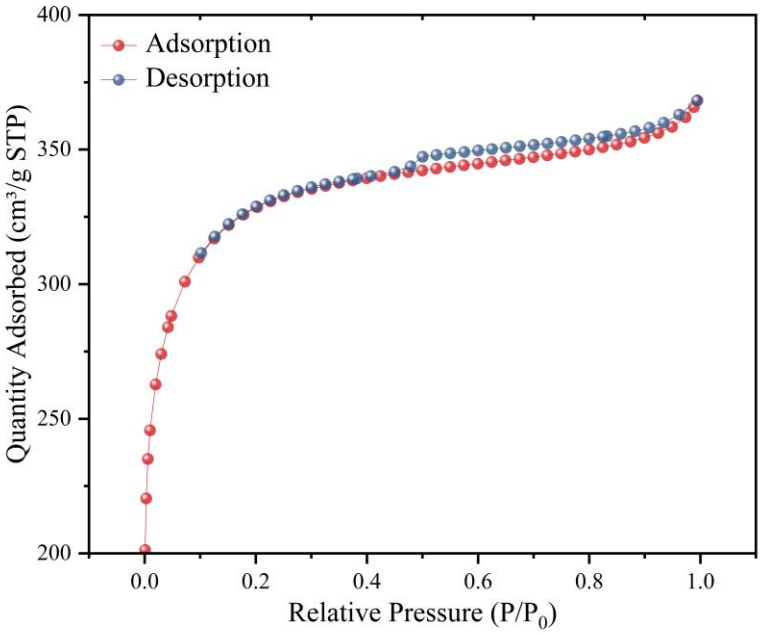

Fig. S1. Nitrogen adsorption-desorption isotherms of coconut carbon.

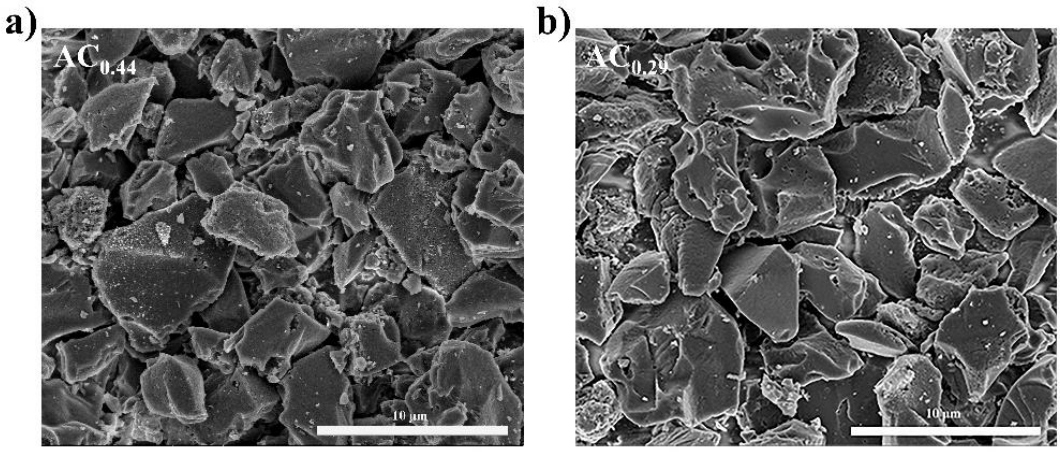

Fig. S2. SEM images of (a) $AC_{0.44}$ and (b) $AC_{0.29}$.

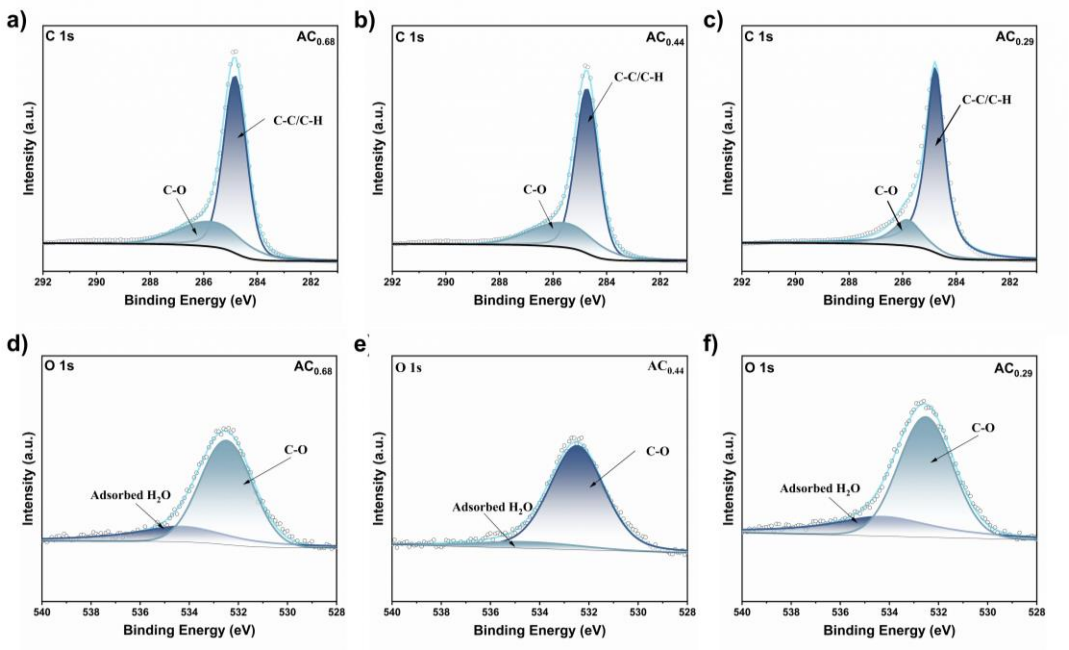

Fig. S3. (a, b, c) XPS high-resolution C 1s and (d, e, f) O 1s spectra of $AC_{0.68}$, $AC_{0.44}$ and $AC_{0.29}$.

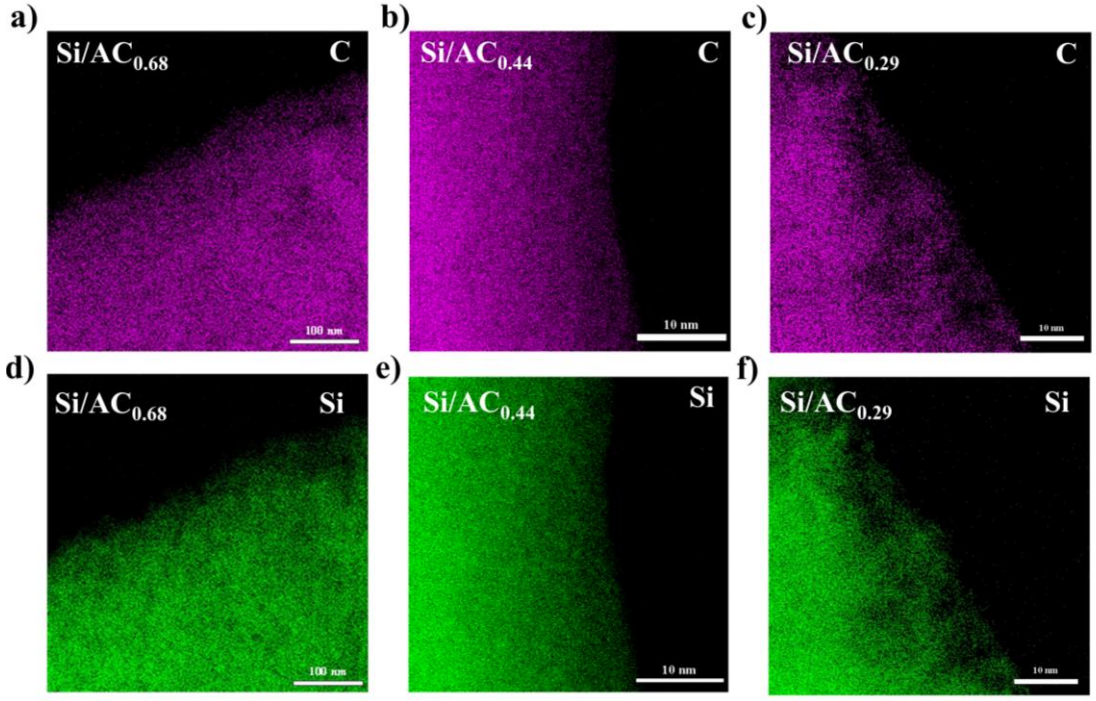

Fig. S4. EDS mapping images of C in $Si/AC_{0.68}$, $Si/AC_{0.44}$ and $Si/AC_{0.29}$ and EDS mapping images of Si in $Si/AC_{0.68}$, $Si/AC_{0.44}$ and $Si/AC_{0.29}$

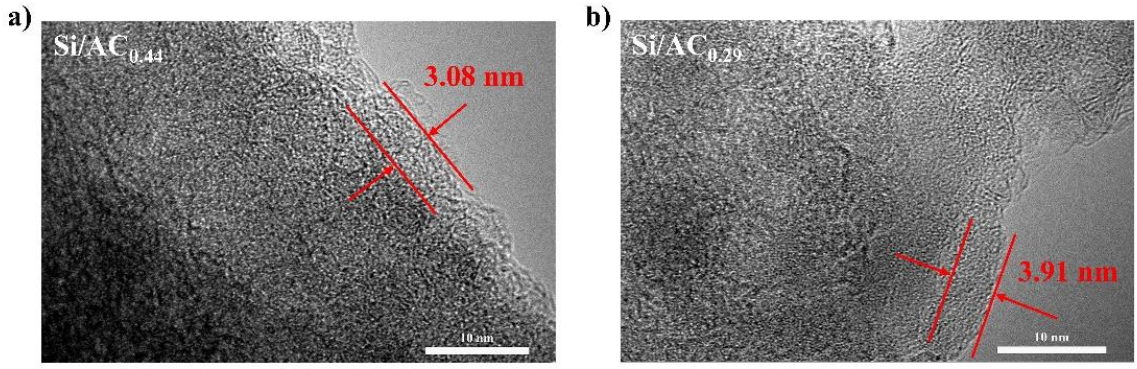

Fig. S5. TEM images of (a) Si/$AC_{0.44}$ and (b) Si/$AC_{0.29}$**.**

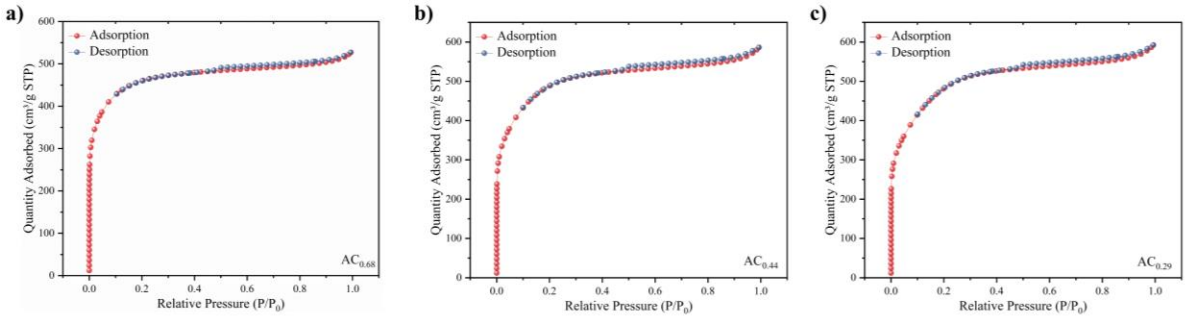

Fig. S6. Nitrogen adsorption-desorption isotherms of (a) $AC_{0.68}$, (b) $AC_{0.44}$ and (b) $AC_{0.29}$.

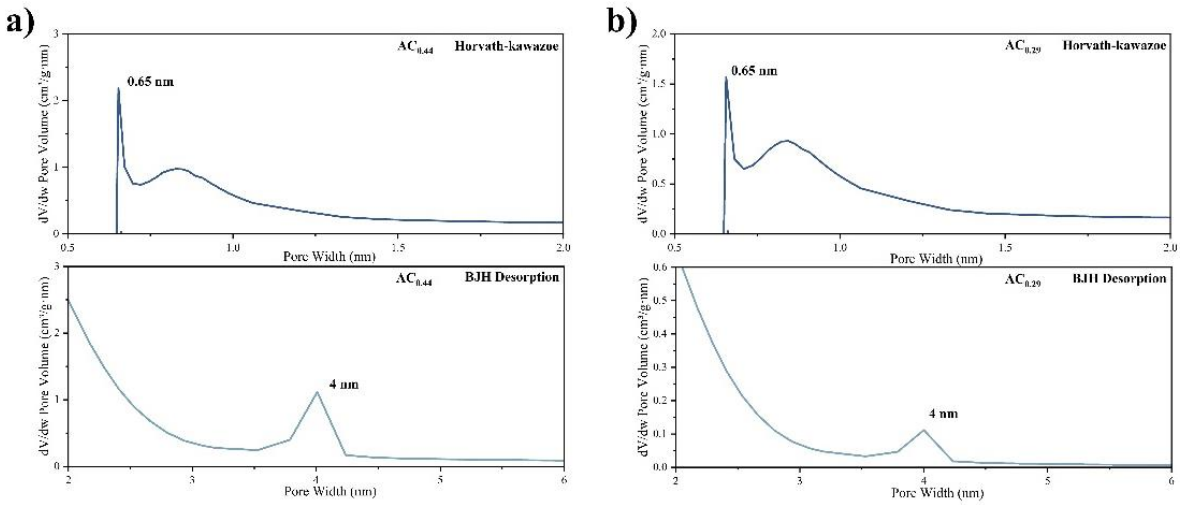

Fig. S7. Pore size distribution of (a) $AC_{0.44}$ and (b) $AC_{0.29}$.

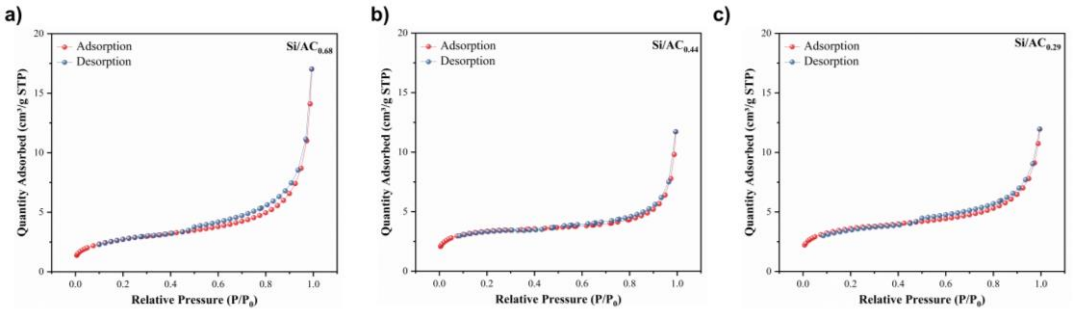

Fig. S8. Nitrogen adsorption-desorption isotherms of the (a) Si/$AC_{0.68}$, (b) Si/$AC_{0.44}$ and (b) Si/$AC_{0.29}$.

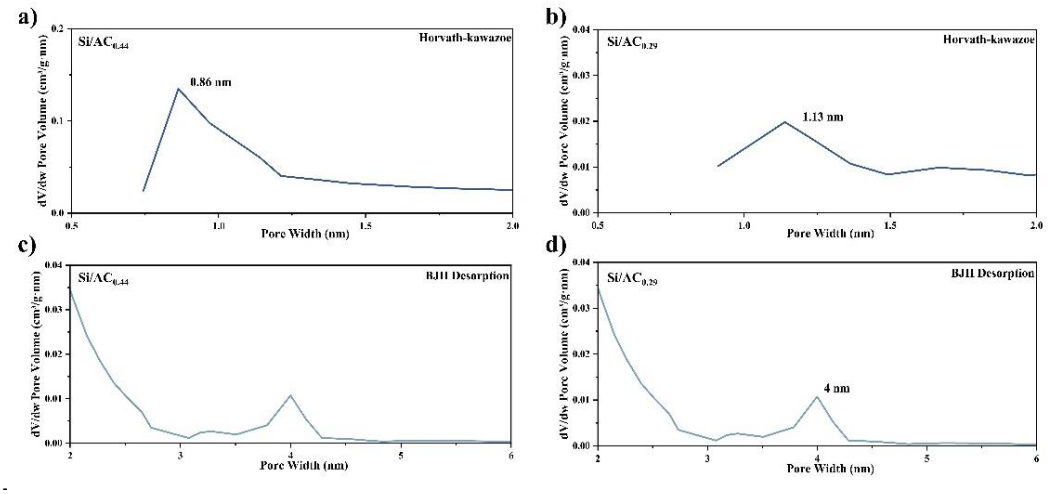

Fig. S9. (a, b)Micropores distribution of $Si/AC_{0.44}$ and $Si/AC_{0.29}$ calculated by the Horvath-Kawazoe model. (c, d) Mesopores distribution of $Si/AC_{0.44}$ and $Si/AC_{0.29}$ calculated by the BJH model.

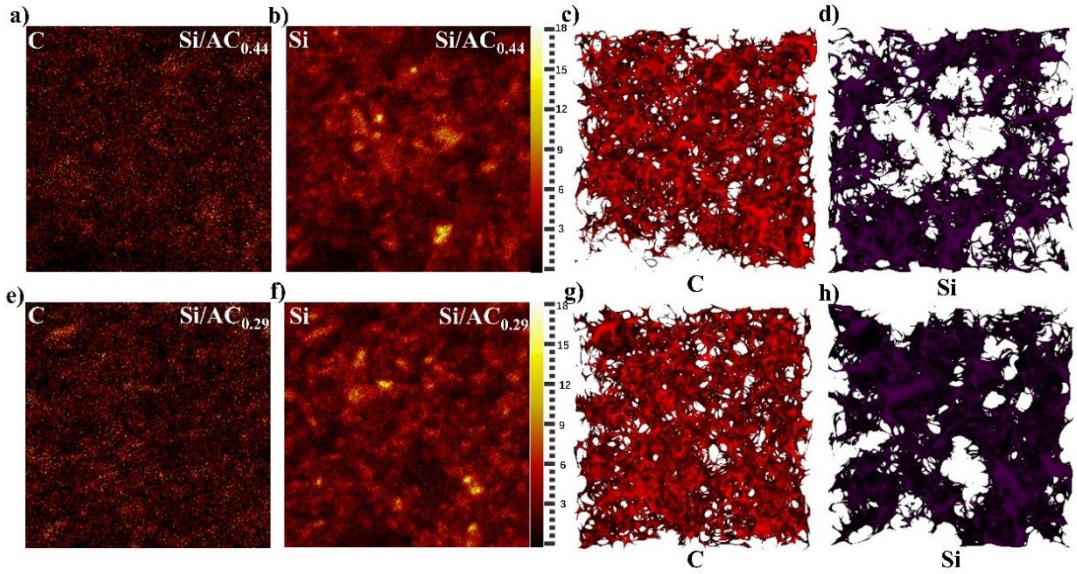

Fig. S10. (a, b) Carbon (C) and Silicon (Si) TOF-SIMS chemical mapping in $Si/AC_{0.44}$. (c, d) TOF-SIMS 3D reconstruction for the sputtered volume of carbon (C) and Silicon (Si) in $Si/AC_{0.44}$. (e, f) Carbon (C) and Silicon (Si) TOF-SIMS chemical mapping in $Si/AC_{0.29}$. (g, h) TOF-SIMS 3D reconstruction for the sputtered volume of carbon (C) and Silicon (Si) in $Si/AC_{0.29}$.

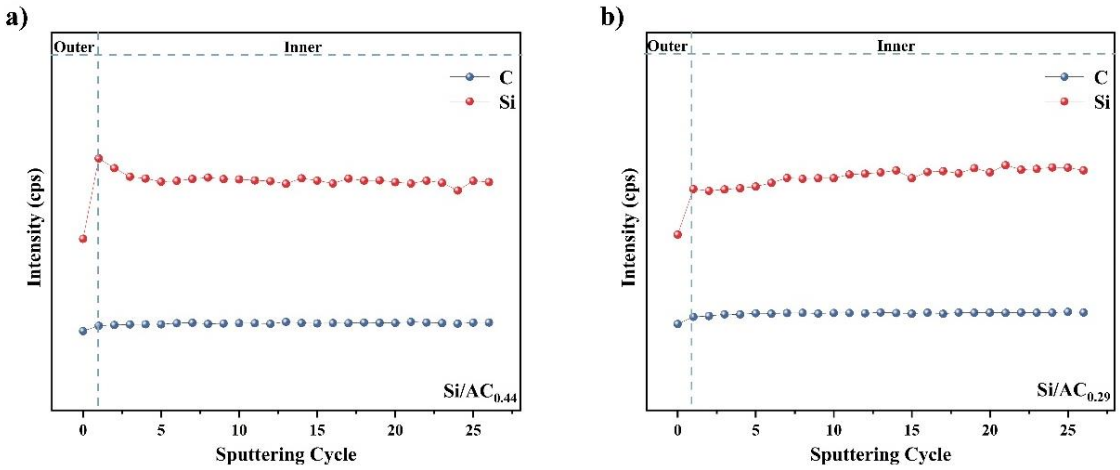

Fig. S11. (a, b) Depth profiles of Carbon (C) and Silicon (Si) signals in $Si/AC_{0.44}$ and $Si/AC_{0.29}$**.**

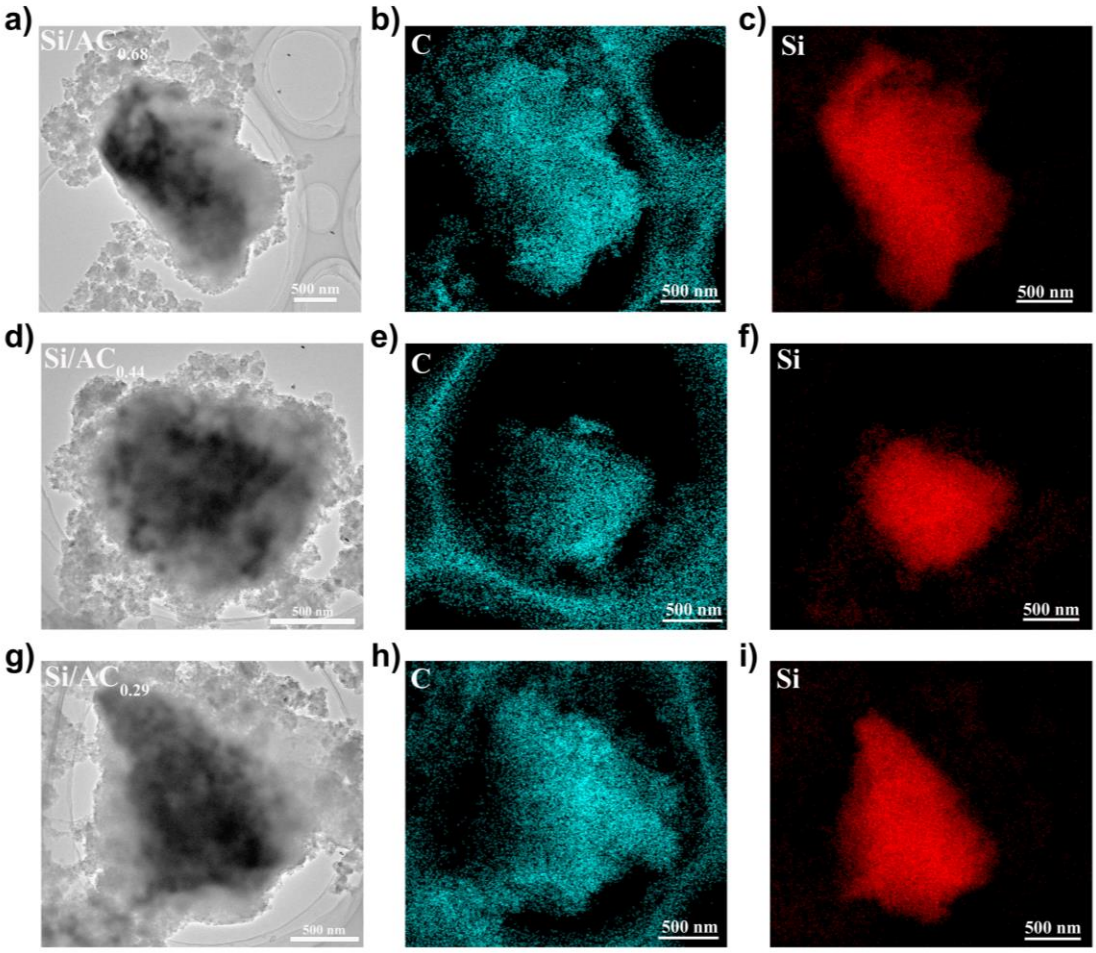

Fig. S12. (a) Post-cycling TEM images and EDS mapping images of (b) C and (c) Si in $Si/AC_{0.68}$. (d) Post-cycling TEM images and EDS mapping images of (e) C and (f) Si in $Si/AC_{0.44.}$ (g) Post-cycling TEM images and EDS mapping images of (g) C and (h) Si in $Si/AC_{0.29}$.

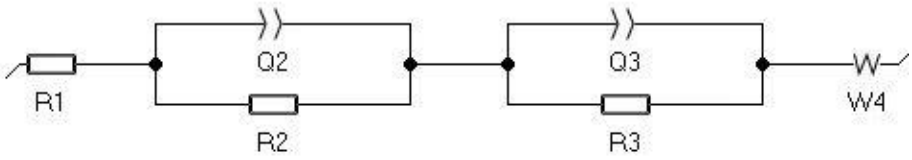

Fig. S13. Equivalent circuit model for EIS data analysis.

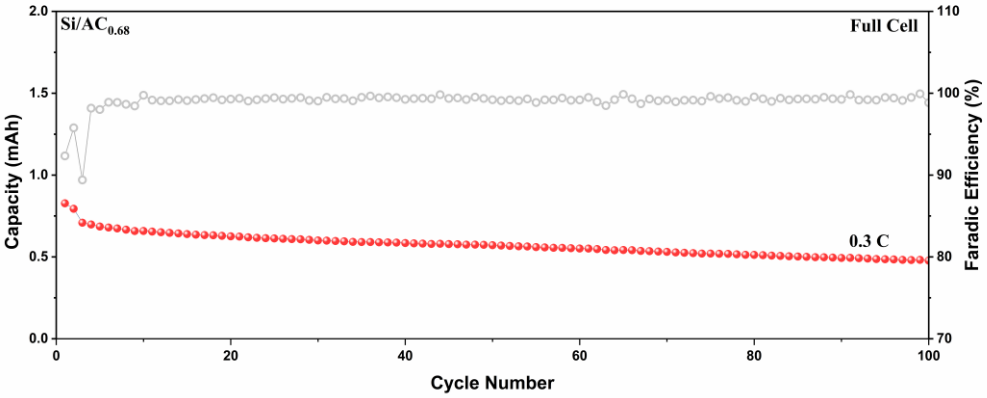

Fig. S14. Full-cell cycling performance at 0.3 C rate.

Table S1. The BET surface area, t-plot micropore area, BJH desorption cumulative surface area, single point desorption total pore volume and the micropore surface area to BET surface area ratios of the $AC_{0.68}$, $AC_{0.44}$ and $AC_{0.29}$.

Samples	BET Surface Area ($m^2\ g^{-1}$)	t-plot Micropore Area ($m^2\ g^{-1}$)	BJH Desorption Cumulative Surface Area ($m^2\ g^{-1}$)	Single Point Desorption Total Pore Volume ($cm^3\ g^{-1}$)	$S_{Micropore}/S_{BET}$ (%)
$AC_{0.68}$	1727.6	1179.8	485.1	0.84	68.3
$AC_{0.44}$	1771.1	869.3	769.1	0.89	44.1
$AC_{0.29}$	1708.8	494.1	1018.4	0.91	28.9

.

Table S2. O, N and H content of the $AC_{0.68}$, $AC_{0.44}$ and $AC_{0.29}$.

Samples	O	N	H
$AC_{0.68}$	7.04405	0.38551	0.41581
$AC_{0.44}$	10.79259	0.31964	0.64183
$AC_{0.29}$	7.61062	0.38599	0.67108

Table S3. Peak positions and their corresponding chemical bonds.

Samples	C 1s	C 1s	O 1s	O 1s
	C-C/C-H	C-O	C-O	Adsorbed H_2O
$AC_{0.68}$	284.83 eV	285.72 eV	532.49 eV	534.3 eV
$AC_{0.44}$	284.73 eV	285.62 eV	532.49 eV	534.5 eV
$AC_{0.29}$	284.78 eV	285.83 eV	532.53 eV	534.28 eV

Table S4. The BET surface area, t-plot micropore area, BJH desorption cumulative surface area and single point desorption total pore volume of the $Si/AC_{0.68}$, $Si/AC_{0.44}$ and $Si/AC_{0.29}$.

Samples	BET Surface Area (m^2 g^{-1})	t-plot Micropore Area (m^2 g^{-1})	BJH Desorption Cumulative Surface Area (m^2 g^{-1})	Single Point Desorption Total Pore Volume (cm^3 g^{-1})
$Si/AC_{0.68}$	12.4787	7.3677	6.0826	0.018124
$Si/AC_{0.44}$	12.3770	7.9382	5.4700	0.016292
$Si/AC_{0.29}$	13.1246	5.9135	8.9514	0.018506

Table S5. Slope and residual sum of squares of the fitted curves derived from the TOF-SIMS depth profile data in $Si/AC_{0.68}$, $Si/AC_{0.44}$ and $Si/AC_{0.29}$.

Samples	Slope	Residual Sum of Squares
$Si/AC_{0.68}$	9.70751±4.25934	321294.06324
$Si/AC_{0.44}$	-15.92716±6.72115	8000028.25635
$Si/AC_{0.29}$	53.18295±6.88162	838686.18069